

## APPLICATION OF CERAMIC INJECTION MOULDING AND PRESSURE INFILTRATION TO THE MANUFACTURING OF ALUMINA/AlSi10Mg COMPOSITES

Ceramic injection moulding and gas pressure infiltration were employed for the manufacturing of alumina/AlSi10Mg composites. Porous ceramic preforms were prepared by mixing alumina powder with a multi-binder system and injection moulding of the powder polymer slurry. Then, the organic part was removed through a combination of solvent and thermal debinding, and the materials were finally sintered at different temperatures. The ceramic preforms manufactured in this way were infiltrated by an AlSi10Mg alloy. The microstructure and properties of the manufactured materials were examined using scanning electron microscopy, mercury porosimetry and bending strength testing. The results of transmission electron microscopy and scanning electron microscopy observations show that the fabricated composite materials are characterised by the percolation type of the microstructure and a lack of unfilled pores with good cohesion at the metal-ceramic interfaces. This is surprising considering that over 30% of the pores are smaller than 1  $\mu\text{m}$ . The results show that the bending strength of the obtained composites decreased with increasing sintering temperature of the porous preforms.

*Keywords:* composite materials, pressure infiltration, ceramic injection moulding, aluminium alloy,  $\text{Al}_2\text{O}_3$

### 1. Introduction

The combination of aluminium alloys and ceramic materials produces a group of materials known as aluminium matrix composites, which have been widely studied since the 1920s and now are used, for example, in the automotive industry. This material offers a large variety of mechanical properties depending on the chemical composition of the matrix alloy and the reinforcing phase, which is predominantly alumina or silicon carbide. Ceramics exhibit brittle behaviour, lacking the necessary fracture toughness for most heavy-duty applications. In contrast, low-density metallic materials, such as aluminium and magnesium and their alloys, which possess the desired fracture toughness, show low strength at temperatures above 250°C. Thus, for such applications, a composite material combining the desirable properties of the two different phases might be vastly superior [1,2].

The pressure infiltration of liquid metal is one of the most important processing routes for the production of aluminium matrix composites with a reinforcement phase. The production process of these materials consists of pushing the molten metal into the open pores of sintered preforms using pressurised inert gas. This method combines the techniques of casting (infiltration process) and powder metallurgy (preparation of porous sintered preforms). The pressure infiltration process allows the development of various composite materials with a continu-

ous nature of reinforcement or the possibility of local product reinforcement. The base of composite materials produced by the infiltration process is a porous sintered preform that affects the structure and thus the final properties of the material. The structure should be created by the open pores that are connected and form canals, allowing the easy flow of molten metal during infiltration. The properties of the porous ceramics, the metal melt and their interactions are most important regarding the resulting material properties [3-7].

The most important limitation on the production of ceramic-metal composites using molten metal infiltration resides upon the compatibility of the reinforcement and the matrix. The thin oxide layer impedes the surface wetting of the ceramic preform by a liquid metal. Therefore, they have used aluminium alloys with magnesium additives, which causes “cracking” of the oxide layer and improves the wettability. One method of manufacturing the modern porous materials intended for pressure infiltration is injection moulding of ceramic powders (known as ceramic injection moulding (CIM)). CIM allows the manufacturing of complex dimensional parts with narrow dimensional tolerances. The mould design and injection parameters highly influence the properties of the finished product. The CIM process usually contains four necessary steps: forming a feedstock of powder-binder mixture, shaping the feedstock using an injection moulding machine, degradation of the binder and densification in the sintering process. In the injection moulding of ceramic

\* SILESIAAN UNIVERSITY OF TECHNOLOGY, INSTITUTE OF ENGINEERING MATERIALS AND BIOMATERIALS, 18 A KONARSKIEGO STR., 44-100, GLIWICE, POLAND

# Corresponding author: grzegorz.matula@polsl.pl

powders, the powder is mixed with a binder. A perfect binder system for CIM must have good flow characteristics, interaction with the powder, debinding and manufacturing. The optimal binder should have a low contact angle and a low viscosity at the moulding temperature, and also adhere to the powder during the moulding process. The binder system has to be fully decomposed before sintering. However, the sample must hold the shape during debinding. For the manufacturing system, the binder must be cheap and environmental friendly [8-12].

The primary objective of this study was to design a manufacturing method and study the structure and properties of aluminium matrix composites reinforced by sintered porous preforms based on  $\text{Al}_2\text{O}_3$ .

## 2. Materials and experimental procedure

The composite material used in this study was produced by pressure infiltration, which consisted of liquid metal and a porous ceramic preform. Aluminium alloy EN AC- $\text{AlSi10Mg(a)}$  was used as a matrix, while as reinforcements, the  $\text{Al}_2\text{O}_3$  preforms produced by CIM, degradation and sintering process of Nabalox NO-115 powder with the addition of polymers and paraffin wax being a pore forming agent. The chemical composition of the aluminium alloy is presented in Table 1. The alumina powder NABALOX NO-115 used in this work was produced by Nabaltec (Germany). The chemical composition of the  $\text{Al}_2\text{O}_3$  powder is shown in Table 2. The morphology observation carried out using scanning electron microscopy (SEM, SUPRA 35, ZEISS) proved that the alumina powder has an irregular shape, as shown in Fig. 1. Particle size distribution measurements were performed by means of a particle size analyser, ANALYSETTE 22 MicroTec plus, FRITSCH, which showed that particle size is less than 20  $\mu\text{m}$  (Fig. 2).

TABLE 1

Chemical composition of aluminium alloy EN AC- $\text{AlSi10Mg(a)}$ 

Mean mass concentration of elements, wt.%							
Si	Fe	Cu	Mn	Mg	Cr	Others	Al
10.6	0.26	0.02	0.28	0.30	0.01	0.042	Bal.

TABLE 2

Chemical composition of as-received NABALOX NO-115 powder

Chemical composition	$\text{Al}_2\text{O}_3$	$\text{Fe}_2\text{O}_3$	$\text{NaO}_2$
wt. [%]	99.5	0.1	0.4

The manufacturing process of ceramic preforms, which are the reinforcement of composite materials, have been produced in four steps:

- preparation of a mixture of  $\text{Al}_2\text{O}_3$  powder with a binder,
- injection moulding of the prepared powder-polymer slurry,
- debinding of the organic components,
- sintering.

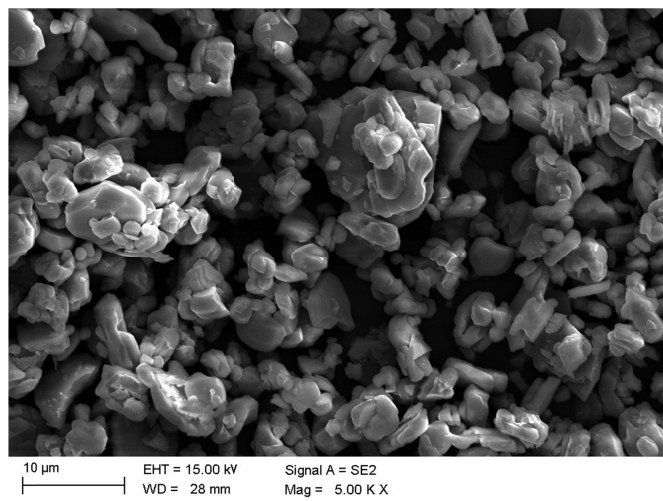


Fig. 1. Morphology of as-received NABALOX NO-115 powder

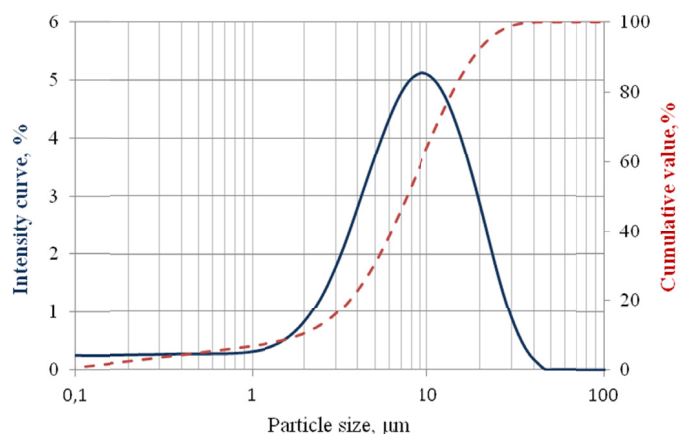


Fig. 2. Particle size distribution of as-received NABALOX NO115 powder

In the first step, the ceramic powder was mixed with the binder based on a polymer (polypropylene (PP)/ polyethylene (HDPE)), paraffin wax (PW) and stearic acid (SA). The composition of the powder-binder mixture is presented in Table 3. The powder-binder mixture was mixed using an extruder machine to obtain a homogeneous mixture.

TABLE 3

Composition of feedstock

	$\text{Al}_2\text{O}_3$	PP	HDPE	PW	SA
%vol.	50	11	11	22	6
%wt.	80.89	4.14	4.33	8.30	2.34

In the next step, feedstock was injected into a rectangular shape three-plate mould ( $4 \times 11 \times 62$  mm). Processing parameters, such as temperature, injection speed pressure and volume, were selected to ensure complete filling of the mould, as carried out based on previous work [13].

The debinding process was performed to remove the organic components (polymers, PW and SA) from the sample after the

injection step. The organic part was removed through the combination of solvent and thermal debinding. In order to reduce the total time of thermal debinding, samples were immersed in heptane at 60°C for 1 h. Heptane was used to dissolve mainly PW and SA. The degradation and sintering temperature was selected experimentally [14] by thermogravimetric analysis (TGA) of the individual binder components. TGA was necessary to determine the initial and final decomposition temperature of the material used in the study (Fig. 3). Samples were sintered for 1 h at different temperatures from 1200 to 1600°C without protective gas (airflow of 3 l/min) and using heating a rate of 1°C/min, as shown in Figure 4. After sintering, the porosity of ceramic performs was measured by mercury porosimetry.

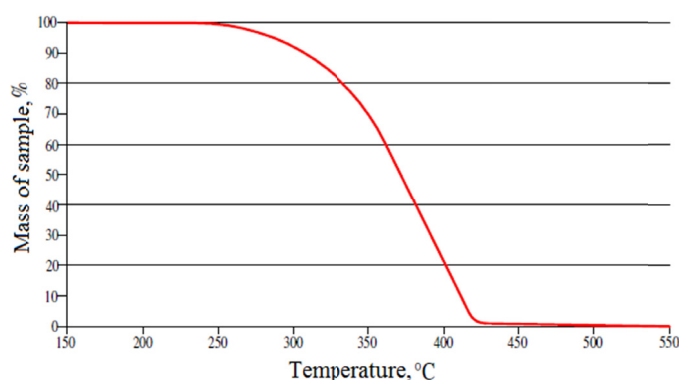


Fig. 3. TGA of PP with heating rate of 7.5 to 550°C in air

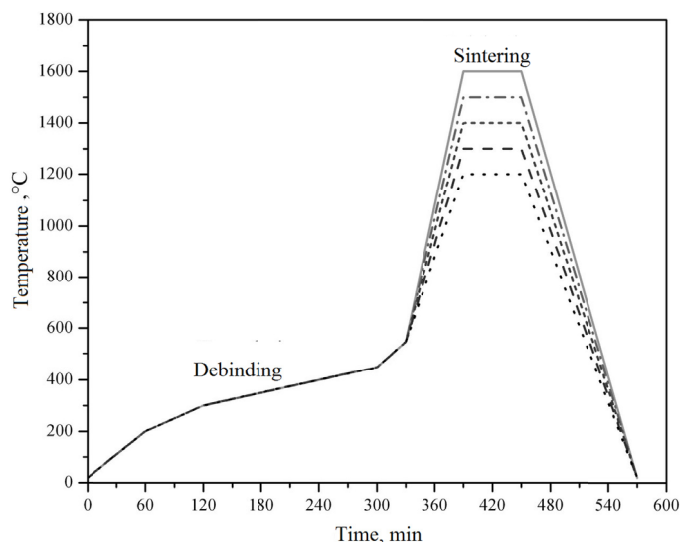


Fig. 4. Scheme of sintering process

The fabrication of infiltrated composites was done using an apparatus for gas pressure infiltration of porous materials (PTA-8/PrGC2P) produced by CZYLOK. The sintered, porous preforms were fixed to a movable plunger, located in the upper part of the infiltration device. An AlSi10Mg ingot was put into the silicon carbide crucible, which was placed in the lower section of the infiltration chamber. As soon as the preform and crucible were inserted, the chamber was closed and vacuumed

to 50 mbar. The crucible was heated up to 800°C. After 60 min, the plunger with the samples was put into the molten alloy and the nitrogen was released. Three different pressures of nitrogen were used (1, 2 and 3 MPa). After 180 s, the plunger with the obtained composite samples was raised up, and the gas was removed from the chamber. Then, the samples were removed from the chamber and cooled down with compressed air.

The observation of the microstructure of the composite materials was carried out using a light microscope LEICA MEF4A and a scanning electron microscope ZEISS Supra 35 with EDS microanalysis. The specimens for metallographic observation were prepared by grinding through 120-1200  $\mu\text{m}/\text{mm}^2$  papers and polishing with 6, 3 and 1  $\mu\text{m}$  diamond paste. To determine the mechanical properties of the manufactured composite materials, a three-point bending test on a ZWICK Z050 universal testing machine was performed.

### 3. Results and discussion

The morphology of the fabricated porous alumina samples is shown in Fig. 5. The microscopic observations reveal relatively small and irregular pores occurring near to sintered alumina particles. Defects, such as gas bubbles, cracks or clusters of pores formed after binder degradation did not occur. Analysis of ceramic fractures also showed the effect of higher sintering temperatures on the alumina particles consolidation by the formation of necks. In addition, it can be seen that the higher sintering temperature affects the rounding off the edges of ceramic particles.

The porosity of the porous  $\text{Al}_2\text{O}_3$  samples sintered at different temperatures obtained using mercury porosimetry is shown in Table 4. The porosity of the samples seems to be sufficient for liquid metal infiltration because most of the preforms (even sintered at highest temperature) have ~50 vol.% porosity. The sintered preforms at 1200°C are characterised by the smallest share of the ceramic phase and therefore the highest porosity of 50.7 vol.%. By increasing the sintering temperature, the porosity of the sintered alumina samples decreases to 46.5 vol.%. Additionally, based on porosimetric measurements, information on the real density and specific surface area of the corundum samples was obtained. The highest real density of 3.89  $\text{g}/\text{cm}^3$  is for samples sintered at 1600°C, while those sintered at 1200°C

TABLE 4

Porosity and distribution of pore sizes of fabricated ceramic preforms vs. sintering temperature

Properties	Sintering temperature, °C				
	1200	1300	1400	1500	1600
Specific surface area, $\text{m}^2/\text{g}$	1.09	1.01	0.97	0.85	0.76
Median of pore diameter, $\mu\text{m}$	1.30	1.36	1.37	1.36	1.39
Apparent density, $\text{g}/\text{cm}^3$	1.86	1.88	1.89	2.00	2.10
Real density, $\text{g}/\text{cm}^3$	3.78	3.79	3.83	3.86	3.89
Porosity, %	50.7	50.6	50.6	48.1	46.5

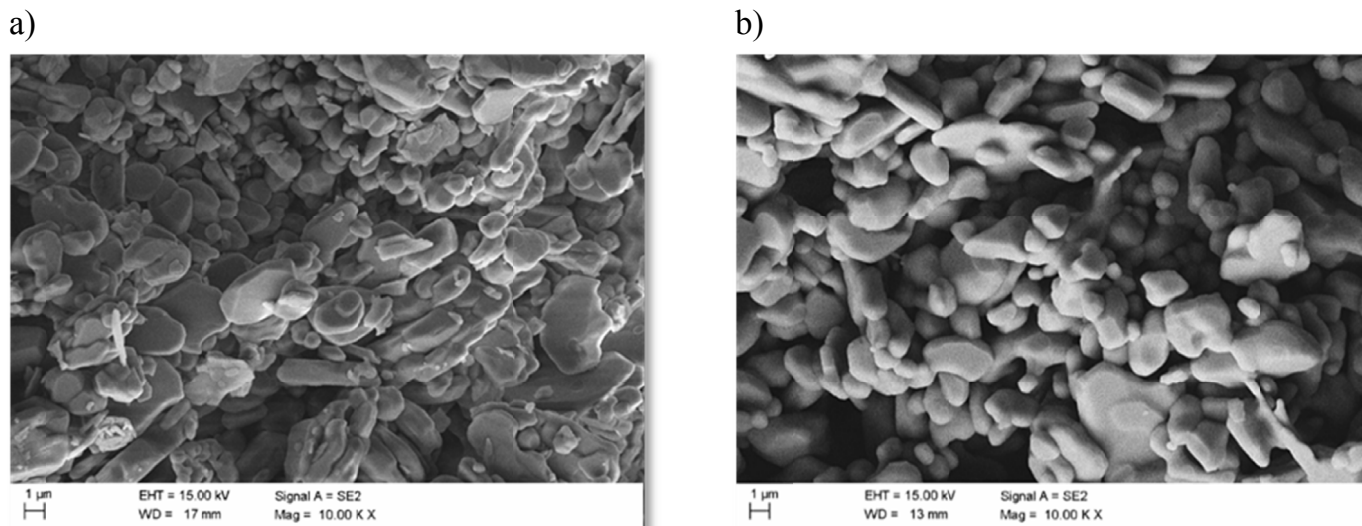


Fig. 5. SEM images of the fracture surfaces of samples sintered at a) 1200 and b) 1600°C

have the lowest real density of 3.79 g/cm<sup>3</sup>. The samples sintered at 1200°C have a specific surface area of 1.09 m<sup>2</sup>/g, while 0.76 m<sup>2</sup>/g was found for the samples sintered at 1600°C. The distribution of the pore size obtained using mercury porosimetry is presented in Fig. 6. Over 60 vol.% of pores have a size in the range from 1 to 6 µm and what is essential is that 30 vol.% of pores have a size less than 1 µm.

Metallographic observation (Fig. 7) shows that composite materials infiltrated under a pressure of 3 MPa are characterised by a very regular distribution of sintered alumina particles, percolation type of the microstructure and the lack of unfilled pores and with good cohesion at the metal-ceramic interfaces. Almost all pores were filled with liquid aluminium alloy. Additionally, it can be noticed that even micro spaces created at the boundaries of the alumina particles were filled by molten alloy tightly. The interface presented in the Fig. 8 between the aluminium alloy and the alumina ceramics are compact and continuous along the

entire cross-section. No delamination and voids at the interface were observed.

Figure 9 shows the three-point bending strengths relating to the different sintering temperatures of the alumina preform and pressure of infiltration. The bending strength of the fabricated composites decreased from 582.5 to 357.3 MPa by increasing the sintering temperature from 1200 to 1600°C. All obtained values are relatively high compared to the bending strength of the unreinforced AlSi10Mg alloy, which is 236 MPa. Although the difference between the aluminium alloy content in particular composites is small (50-46 vol.%), the bending strength results are surprisingly diverse. A reverse phenomenon is demonstrated in previous works [15-18], where it has been demonstrated that with the increase in the content of the aluminium alloy matrix, the bending strength dropped. This difference can be explained by the presence of composites sintered at higher temperatures of closed pores, which during infiltration have not been filled

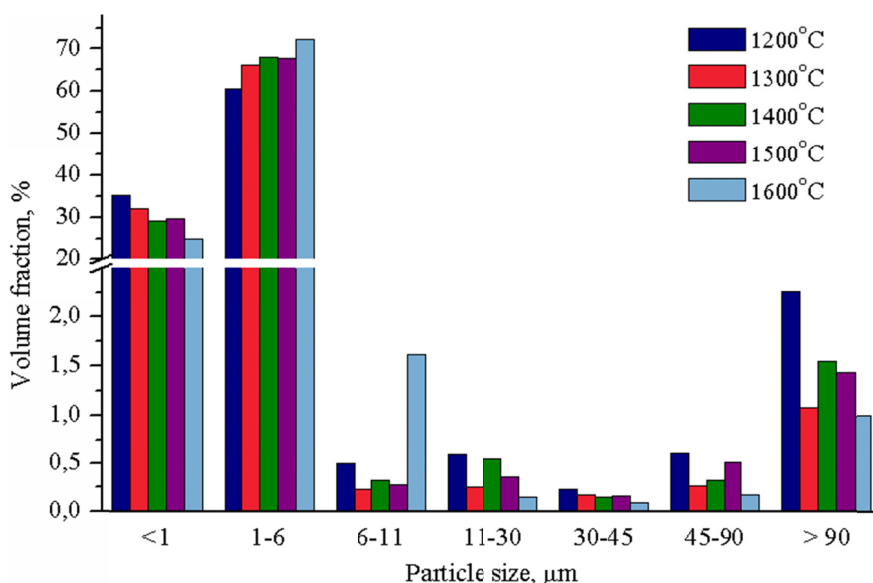


Fig. 6. Distribution of pore sizes in sintered alumina preforms

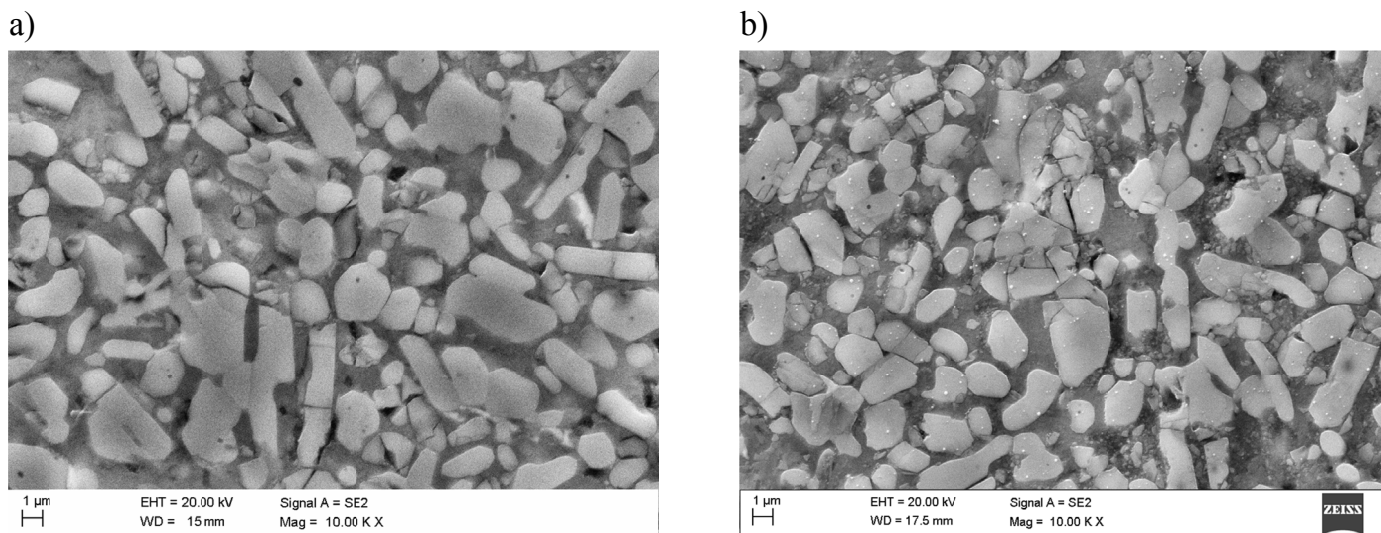


Fig. 7. Microstructure of infiltrated composite materials reinforced with ceramic preforms sintered at a) 1200°C and b) 1600°C, SEM

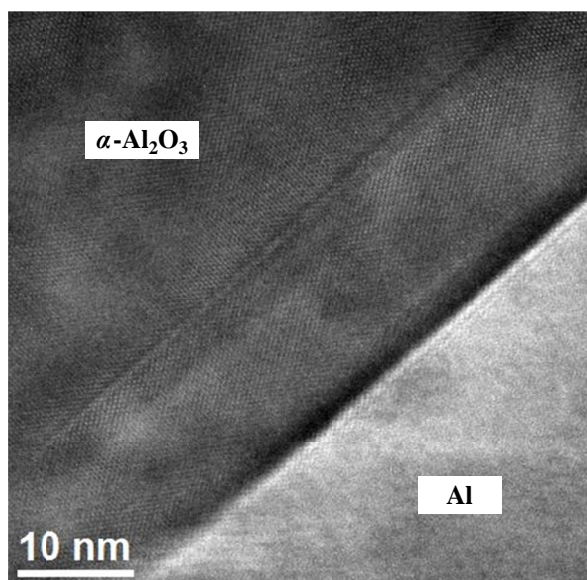


Fig. 8. Microstructure of infiltrated composite reinforced with alumina preform sintered at 1600°C, TEM

with a liquid alloy, thus affecting negatively on the mechanical properties. The use of CIM and the sintering process for the porous samples caused only a slight sintering shrinkage ranging from 1 to 5%. Such a low shrinkage with a binder content of 50% suggests that the primary mechanism of free sintering is surface diffusion, causing neck growth between contacting particles. This type of mass transfer is characteristic of a low sintering temperature, which is  $0.7\times$  the melting point, according to the literature. Assuming that the melting point of  $\text{Al}_2\text{O}_3$  is 2030°C, 70% of this temperature is  $\sim 1420^\circ\text{C}$ .

An important factor is also the amount of binder, which is necessary to the injection moulding process. Conventionally compressed powders are much more packed than injection moulded ones. Hence, connections between particles (the so-called necks) occur less frequently than in compressed and sintered materials. As shown by microscopic studies during production, there was also no increase in the size of grains in alumina sinters. The loosely packed particles give the possibility of easier infiltration in comparison to compressed powders. Bending tests

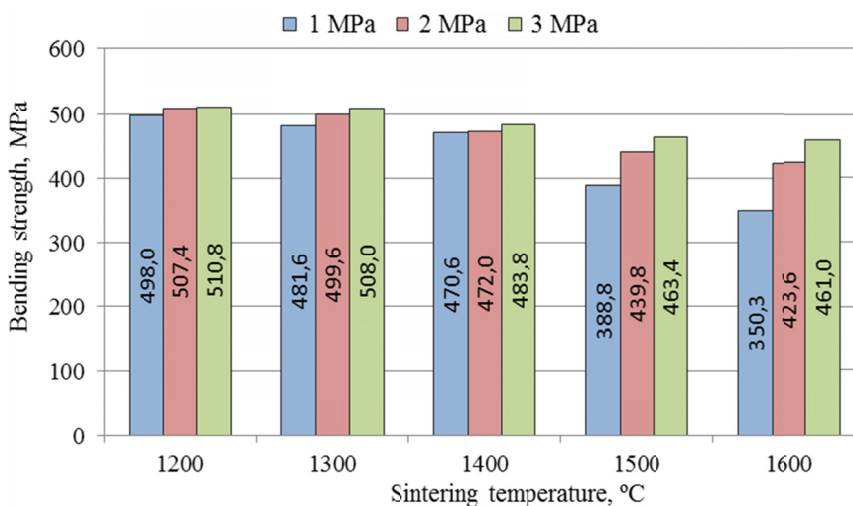


Fig. 9. Effect of sintering temperature and infiltration pressure on bending strength of fabricated composite samples

were carried out also for composite materials infiltrated at the different pressures from 1 to 3 MPa. It can be seen that there is a relation between bending strength and sintering and pressure. This depends on higher sintering temperature, which is the cause of better compaction of the ceramic preform and reduces the porosity due to the stronger diffusion and the formation of necks between sintered powder particles. At lower temperatures, the effect is the opposite, the density of the preform decreases and the porosity increases. It can also be noticed that as the sintering temperature increases, the difference between the bending strength of the composite materials produced at different infiltration pressures becomes more apparent. This phenomenon is most likely related to the presence in samples sintered at higher temperatures, pores which are closed or so small that a liquid alloy does not wet them at a lower pressure. It should be assumed that the higher sintering temperature results in the closing of some pores and the narrowing of the capillary channels by more intense diffusion of atoms. These changes may cause the worse access for liquid metal during pressure infiltration especially at low pressures, resulting in lower bending strength of infiltrated sintered preforms at higher temperatures. This explanation correlates with the results of mercury porosimetry.

#### 4. Conclusions

$\text{Al}_2\text{O}_3$  /AlSi10Mg composites were fabricated by ceramic injection moulding and a gas pressure infiltration technique. The fabricated composites are characterised by the uniform distribution of the reinforcing phase in the metal matrix and exhibited high mechanical properties. The bending strength of the obtained composites decreased with increasing sintering temperature of porous preforms. The highest bending strength of 510 MPa is measured for the composite sintered at 1200°C and infiltrated under a pressure of 3 MPa. Improved strength of the composites was described by strong interfacial bonding between  $\text{Al}_2\text{O}_3$  and the aluminium alloy.

#### Acknowledgements

This publication was financed by the Ministry of Science and Higher Education of Poland as the statutory financial grant of the Faculty of Mechanical Engineering SUT.

#### REFERENCES

- [1] K.U. Kainer, *Metal Matrix Composites*, Wiley-VCH, Weinheim (2006).
- [2] J.W. Kaczmar, K. Pietrzak, W. Włosiński, *J. Mater. Process. Tech.* **106** (1-3) 58-67 (2000).
- [3] K. Konopka, M. Szafran, *J. Mater. Process. Tech.* **175**, 266-270 (2006).
- [4] L.A. Dobrzański, M. Kremzer, K. Gołombek, *Mater. Sci. Forum.* **591**, 188-192 (2008).
- [5] A. Boczkowska, P. Chabera, A.J. Dolata, M. Dyzia, A. Oziębło, *Metalurgija* **52** (3), 345-348 (2013).
- [6] C. Xiaozhou, W. Chao, X. Xiangxin, C. Gongjin, *Arch. Metal. Mater.* **60** (4), 2493-2497 (2015).
- [7] M. Pawlyta, B. Tomiczek, M. Kujawa, L.A. Dobrzański, B. Bierska-Piech, *Mater. Charact.* **114**, 9-17 (2016).
- [8] B. Hausnerova, D. Bleyan, V. Kasparkova, V. Pata, *Ceram. Int.* **42** (1), 460-465 (2016).
- [9] E. Medvedovski, M. Peltsman, *Adv. Appl. Ceram.* **111** (5-6), 333 (2012).
- [10] K. Golombek, G. Matula, J. Mikula, *Mater. Tehnol.* **51** (1), 163-171 (2017)
- [11] P. Thomas-Vielma, A. Cervera, B. Levenfeld, A. Várez, *J. Eur. Ceram. Soc.* **28** (4), 763-771 (2008).
- [12] L. Poh, C. Della, S. Ying, C. Goh, Y. Li, *Powder Technol.* **328** (1), 256-263 (2018).
- [13] G. Matula, J. Krzyszczyk, *J. Achiev. Mater. Manuf. Eng.* **71** (1), 14-21 (2015).
- [14] G. Matula, J. Krzyszczyk, B. Lipowska, *J. Achiev. Mater. Manuf. Eng.* **67** (1), 32-38 (2014).
- [15] N. A. Travitzky, *J. Mater. Sci.* **36**, 4459-4463 (2001).
- [16] S.N. Chou, J.L. Huang, D.F. Lii, H.H. Lu, *J. Alloy. Compd.* **436**, 124-130 (2007).
- [17] A. Kurzawa, J.W. Kaczmar, *Arch. Foundry Eng.* **17** (1), 103-108 (2017).
- [18] J. Maj, M. Basista, W. Węglewski, K. Bochenek, A. Strojny-Nędza, K. Naplocha, T. Panzer, M. Tatarkova, F. Fiori, *Mat. Sci. Eng. A-Struct.* **715**, 154-162 (2018).